Virology 476 (2015) 298–303

Contents lists available at ScienceDirect

Virology

journal homepage: www.elsevier.com/locate/yviro

Three-dimensional visualization of the *Autographa californica* multiple nucleopolyhedrovirus occlusion-derived virion envelopment process gives new clues as to its mechanism

Yang Shi [a,1], Kunpeng Li [a,1], Peiping Tang [a,b], Yinyin Li [a], Qiang Zhou [a], Kai Yang [a], Qinfen Zhang [a,*]

[a] State Key Laboratory of Biocontrol, School of Life Sciences, Sun Yat-sen University, Guangzhou, China
[b] Hefei National Laboratory for Physical Sciences at the Microscale, and School of Life Sciences, University of Science and Technology of China, Hefei, Anhui, China

ARTICLE INFO

Article history:
Received 18 June 2014
Returned to author for revisions
2 October 2014
Accepted 28 November 2014
Available online 7 January 2015

Keywords:
Baculovirus
Occlusion-derived virion
Microvesicle formation
Envelopment process
Electron tomography

ABSTRACT

Baculoviruses produce two virion phenotypes, occlusion-derived virion (ODV) and budded virion (BV). ODV envelopment occurs in the nucleus. Morphogenesis of the ODV has been studied extensively; however, the mechanisms underlying microvesicle formation and ODV envelopment in nuclei remain unclear. In this study, we used electron tomography (ET) together with the conventional electron microscopy to study the envelopment of *Autographa californica* multiple nucleopolyhedrovirus (AcMNPV) ODV. Our results demonstrate that not only the inner but also the outer nuclear membrane can invaginate and vesiculate into microvesicles and that intranuclear microvesicles are the direct source of the ODV membrane. Five main events in the ODV envelopment process are summarized, from which we propose a model to explain this process.

© 2014 Elsevier Inc. All rights reserved.

Introduction

Baculoviruses are enveloped, rod-shaped, large, closed circular DNA viruses, with nucleocapsids of 250–300 nm in length and 30–60 nm in diameter (Jehle et al., 2006). The hosts in which the baculoviruses are commonly found are the orders *Diptera*, *Hymenoptera* and *Lepidoptera*. During the baculovirus life cycle, two virion phenotypes are produced, namely, budded virion (BV) and occlusion-derived virion (ODV). In these two phenotypes, genetic information and the nucleocapsid proteins are almost identical, and both DNA replication and nucleocapsid assembly of the two phenotypes occur in the virogenic stroma (VS) (Fraser, 1986; Young et al., 1993). However, the origin of envelopes and the envelope composition differ between the two phenotypes (Braunagel and Summers, 1994; Hou et al., 2013). At about 12 h post-infection (p.i.) (Slack and Arif, 2007), nucleocapsids shuttle out of the nucleus and bud through the plasma membrane and, in this way, BVs are enveloped (MacKinnon et al., 1974; Summers and Volkman, 1976). After approximately 20 h p.i. (Slack and Arif, 2007), ODVs form as nucleocapsids are transported to the region between the nuclear membrane and the VS, termed the ring zone (RZ), enveloped, and embedded within a proteinaceous crystal matrix, forming polyhedra or occlusion bodies (Williams and Faulkner, 1997). Based on the number of nucleocapsids within the ODV envelope, baculoviruses can be categorized as single nucleopolyhedroviruses (SNPVs) or multiple nucleopolyhedroviruses (MNPVs). Notably, there is only one nucleocapsid in the BVs of both SNPVs and MNPVs. Once eaten by larvae, ODVs will be released from the occlusion bodies in the alkaline environment of the larval midgut and initiate infection in the midgut epithelium. On the other hand, BVs can bud from infected cells without cell disintegration and initiate the systemic infection of other susceptible tissues (Engelhard et al., 1994; Tanada and Hess, 1976).

The process of BV envelopment at cell surface is similar to other viral envelopment processes (Welsch et al., 2007); however ODV envelopment in nuclei is common only in baculovirus. In early morphogenesis studies of ODV envelopment by transmission electron microscopy (TEM), viral-induced intranuclear microvesicles and membrane fragments were found in nuclei, and nucleocapsids were bound to them (Fraser, 1986; Kawamoto et al., 1977; Stoltz et al., 1973). Moreover, the inner nuclear membranes (INMs) of infected cells bleb fold in and vesiculate (Tanada and Hess, 1976). Fluorescence and immuno-gold labeling of ODV envelope proteins have

* Correspondence to: School of Life sciences, Sun Yat-sen University, Address: Building 415-Room 101, School of Life sciences, Sun Yat-sen University, Xingang West Road 135#, Guangzhou, China, 510275. Tel.: +8620 84112286.
E-mail address: lsszqf@mail.sysu.edu.cn (Q. Zhang).
[1] These authors contributed equally to this work.

http://dx.doi.org/10.1016/j.virol.2014.11.030
0042-6822/© 2014 Elsevier Inc. All rights reserved.

been performed using confocal microscopy and immuno-electron microscopy, respectively. This identified ODV envelope proteins including ODV-E66 (Hong et al., 1994), ODV-E56 (Braunagel et al., 1996), ODV/BV-E26 (Beniya et al., 1998), and Ac76 (Hu et al., 2010; Wei et al., 2014) on the nuclear membranes of infected cells, microvesicles or nucleocapsids associated with membrane fragments, and ODV envelopes. Although phospholipid analysis found distinct differences between ODV envelopes and uninfected Sf9 nuclear membranes (Braunagel and Summers, 1994), a semi-permeabilization assay demonstrated that the cholesterol concentration increased in infected Sf9 cell nuclear envelopes and approached that in the ODV envelope (Braunagel and Summers, 2007). This is considered as that baculovirus infection induces lipid remolding of the nuclear envelope. Taken together, the aforementioned protein positioning and lipid analyses imply that nuclear membranes are the source of ODV envelopes.

However, no direct observation or evidence of a relationship among the nuclear envelope, virus-induced intranuclear microvesicles, and the ODV envelope has been reported. Furthermore, no systematic model has been proposed to explain how the microvesicles envelope nucleocapsids.

In this study, we performed electron tomography (ET) combined with sectioning of plastic-embedded samples to visualize microvesicle formation and ODV envelopment in *Autographa californica* MNPV (AcMNPV), the most widely studied Baculoviridae species, in three dimensions (3D). Based on two-dimensional (2D) observations and visualization of specific areas of interest in 3D, we summarize ODV envelopment and provide a model to explain how the numerous nucleocapsids are enveloped. Moreover, based on our observation, we propose an optional way for microvesicles formation that microvesicles can form via large-scale invagination of double nuclear membranes and vesiculation into single-membrane vesicles.

Results and discussion

We examined more than 300 cells at 24, 36, 48, and 72 h p.i. by conventional TEM and ET. Based on these data, we deduced a model (Fig. 1) to explain how microvesicles form and ODVs are enveloped. Microvesicles are from the invaginated nuclear membrane and the vesiculated nuclear membranes then interact with and envelop nucleocapsids. Thereafter, membranes invaginate and nucleocapsids are separated into different ODVs such that all nucleocapsids in a given ODV are oriented parallel to each other. The various steps of this process are described below. None of these features were observed in non-infected cells.

Formation and maturation of the microvesicles

Among all our data at different time points post-infection, we seldom captured the clear images of invaginating INMs, which is a widely accepted model to explain the origin of microvesicles (Braunagel and Summers, 2007) (labeled as steps A2 and B2 in Fig. 1). However, surprisingly, at 24 and 36 h p.i., not only the INM but also the outer nuclear membrane (ONM) invaginate into the nuclei of infected cells (Fig. 2A–C). Some parts of the inward-folded nuclear membrane form vesicle-like structures (boxed in Fig. 2B). The ONM (indicated by black arrows in Fig. 2B) is noticeably prone to form the vesicle-like structures compared to the INM (indicated by red arrows in Fig. 2B). This process is labeled step A1 in Fig. 1. Moreover, large pieces of intranuclear membranes (Fig. 2D–F) are found within the nuclei in 24 and 36 h p.i. This is labeled steps B1 and C1 in Fig. 1. These intranuclear membranes exhibit vesiculation and are double membranes reminiscent of the invaginating nuclear membrane. This suggests that these intranuclear membranes are derived from the invaginated nuclear membranes. Furthermore, it is

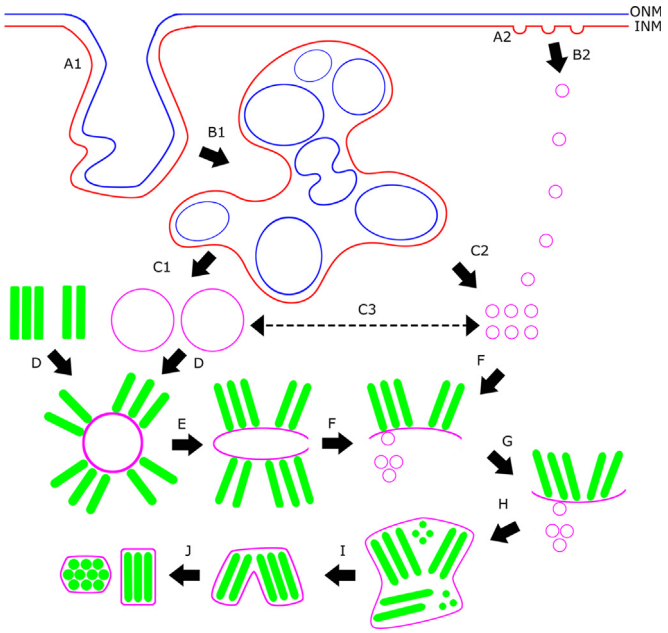

Fig. 1. Schematic model of microvesicle formation and occlusion-derived virion (ODV) envelopment. The outer nuclear membrane (ONM) is in blue, the inner nuclear membrane (INM) in red, large microvesicles, small microvesicles, and ODV membranes in purple, and nucleocapsids in green. (A1) The nuclear membranes (both ONM and INM) fold inwards. Part of the invaginating nuclear membrane sags, especially the ONM. (A2) Only the INM is invaginating. (B1) The invaginated intranuclear membrane vesiculates, and vesicles appear earlier from the ONM than from the INM. (B2) Small microvesicles are formed by invaginating INM. A1 and B1 are the steps based on our data. A2 and B2 are the widely accepted microvesicle formation pathway (Braunagel and Summers, 2007). (C) After a series of complicated steps, intranuclear double membranes can form several single-membrane vesicles that can be categorized as large (C1) and small (C2) microvesicles. They may transform to one another (C3) by fusion and fission. (In the data of our research, we could not validate this process, therefore, we use dashed line to show the C3 step.) (D) Several nucleocapsid bundles adhere to large microvesicles (C1). (E) As more nucleocapsids adhere, the microvesicle deformed and ruptured. Thereafter, the expanding gaps cause the membranes of microvesicles with nucleocapsids attach to become arch-shaped. (F, G) Small microvesicles (C2) continuously fuse with these arch-shaped membranes such that they become large enough to accommodate all the nucleocapsids. (H) The initially formed ODVs contain several nucleocapsid bundles that are not oriented parallel to each other. Thereafter, the membrane invaginates (I) and these bundles separate to form new ODVs (J).

easy to find single-membrane vesicle-like structures (indicated by red arrows in Fig. 2F) are observed around vesiculating intranuclear membranes (indicated by black arrows in Fig. 2F). The diameters, electron densities of the these single-membrane vesicles, together with the thickness of membrane of these vesicles are similar to those of the microvesicles, which are abundant in infected Sf9 cells and are generally accepted to be the origin of ODV membranes. From these results, we infer that microvesicles are derived not only from the INM but also from the ONM. We have summarized the process in a model, comprising steps A1, B1, C1 and C2 (Fig.1). We do not find any of these patterns in non-infected cells.

In previous studies using immuno-gold labeling, ODV membrane proteins were detected on both the INM and ONM (Braunagel et al., 1996; Hong et al., 1997), which does not conflict with our finding that the membranes of microvesicles are derived from both the INM and ONM. Therefore, our model (steps A1 and B1 in Fig. 1) can be an alternative pathway to the previously proposed INM invagination model (steps A2 and B2 in Fig. 1).

Several studies have identified ODV envelopment-related genes. *ac142* (McCarthy et al., 2008) and *ac103* (Yuan et al., 2008) are related to this envelopment, but do not affect nucleocapsid bundling. *ac76* (Hu et al., 2010; Wei et al., 2014) and *ac93* (Yuan et al., 2011) are related to intranuclear microvesicle formation and subsequent ODV

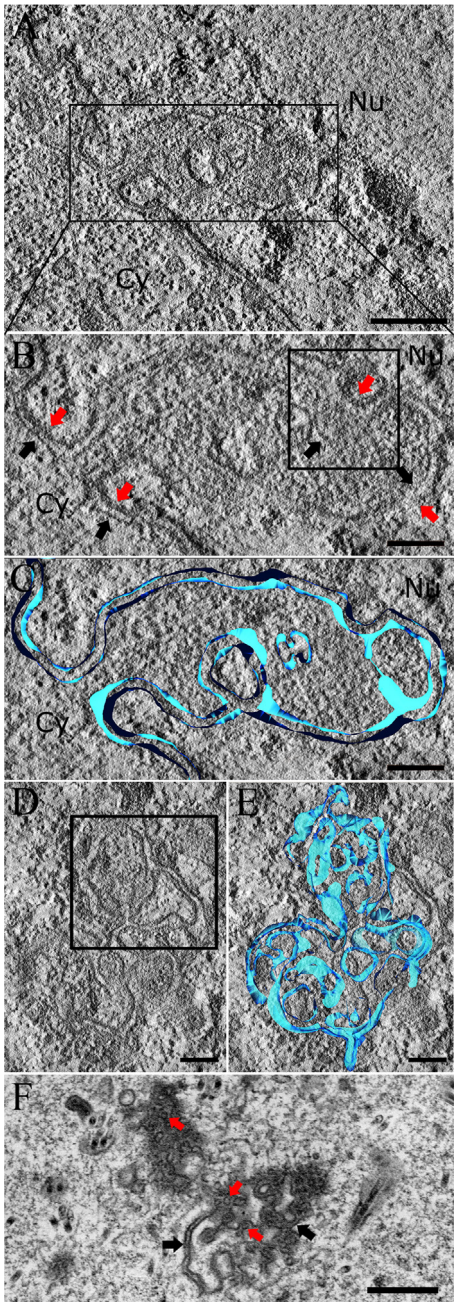

Fig. 2. Electron tomography of the invaginating nuclear membranes and intranuclear membranes of infected Sf9 cells. (A) The inner nuclear membrane (INM) and the outer nuclear membrane (ONM) both fold inwards. (B) High magnification image of the boxed area in (A). Red arrows indicate the INM, and black arrows the ONM. The black box shows a region of the invaginating nuclear membrane that tends to vesiculate. In this case, the ONM has more priority in the vesiculating process. (C) The image shown in (B) with superimposed rendering of the invaginating nuclear membrane. (D) Double membranes are found inside the nucleus. In this example, the ONM-derived membrane has already formed vesicles, while the INM-derived membrane has not. Two vesicles are shown in the box. (E) The image shown in (D) with superimposed rendering of the intranuclear membrane. (F) Two-dimensional micrograph of intranuclear double membranes (indicated by black arrows) vesiculating into several single-membrane microvesicles (indicated by red arrows). In this example, the intranuclear membrane is segmented into several parts, which are at different stages of the vesiculating process. Nu=nucleus, Cy= cytoplasm. Bar=200 nm (B–E), bar=300 nm (A, F). Cells were harvested at 24 h post-infection (p.i.) in A–C and at 36 h p.i. in D–F.

envelopment. Their findings show that the ac76 and ac93 mutants exhibit neither microvesicles nor other types of vesicles, that microvesicles form prior to ODV envelopment and that microvesicles are

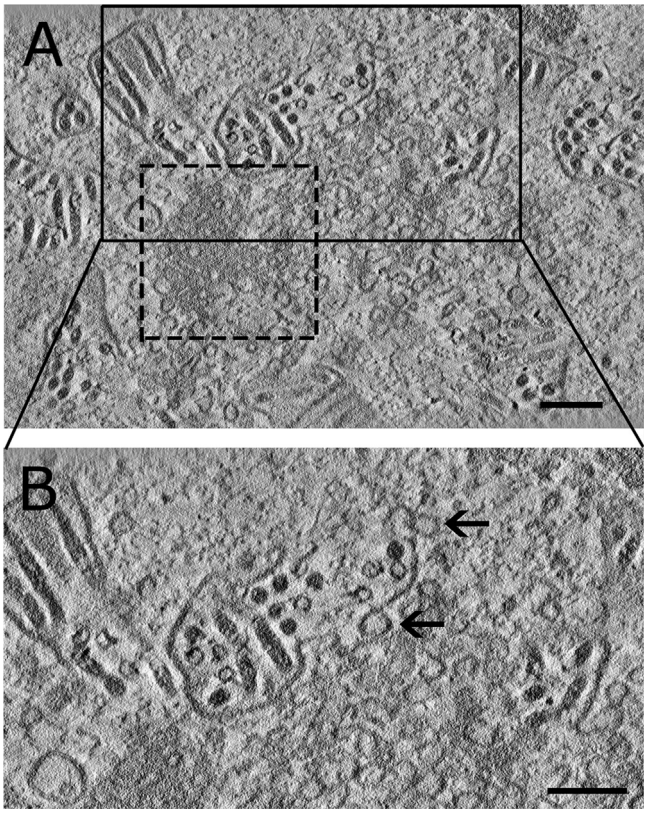

Fig. 3. The relationship between microvesicles and the occlusion-derived virion (ODV) envelope. (A) Enveloping ODVs are surrounded by microvesicles. The dashed box shows the microvesicle foci with a high electron density. (B) Higher magnification image of the boxed area in (A). Arrows indicate microvesicles attached to the envelope of an ODV. Bar =300 nm. In (A) and (B), cells were harvested at 48 h post-infection.

the source of the ODV envelope, as shown in our model. Disruption of these two genes blocks steps A1, A2, B1, B2, C1, and C2 (Fig. 1).

Microvesicles are not evenly scattered throughout the entire RZ rather they tend to cluster in specific areas, especially around the enveloping ODV. In these clusters of microvesicles, there are several foci of microvesicles (Fig. 3) with a high electron density, as previously reported (Braunagel and Summers, 2007). The mean diameter of the microvesicles located inside these foci areas is 44.82 nm ($n=61$, standard deviation (SD)=15.56), while the mean diameter of the microvesicles outside these foci is 93.08 ($n=79$, SD=38.58). Although the SD is quite large because of the non-uniform size of the outside vesicles, microvesicles within the foci are obviously smaller than those outside foci ($P<0.0001$). These data may indicate that the small microvesicles are more stable in the foci and suggest that heterogeneous microvesicles are processed into small microvesicles in these foci (Fig. 1, step C2). In the whole RZ, the size of microvesicles should be dynamic, and both fusion and fission of the microvesicles may happen (Fig. 1, step C3). Anyway, these processes are hard to be distinguished by EM study.

Major sequential events of ODV envelopment

Electron microscopic studies have provided many images of ODV morphogenesis (Fraser, 1986; Knudson and Harrap, 1976; MacKinnon et al., 1974; Tanada and Hess, 1976), but no integrated model of ODV envelopment of MNPV has been proposed. In order to reveal the sequential procedures of ODV envelopment, comprehensive observations on infected cells using conventional TEM and electron tomography were conducted to capture interesting areas of ODV envelopment. All the processes of ODV envelopment were observed

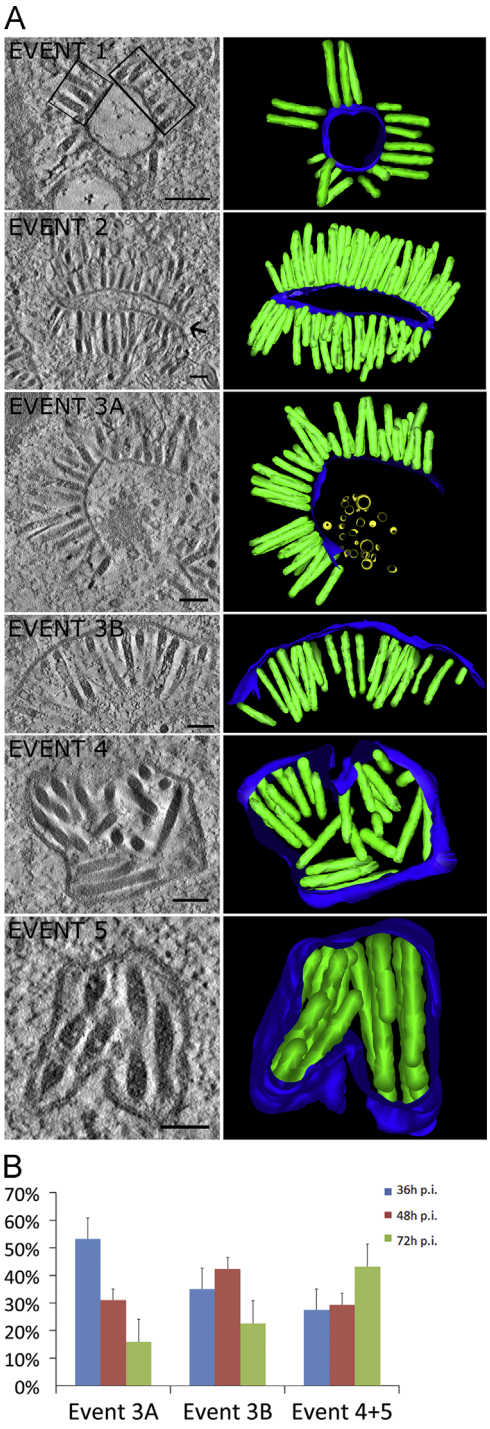

Fig. 4. Main events in the envelopment process as suggested by this study. (A) Images in the right column show 3D rendering of the images in the left column. Membranes in blue, nucleocapsids in green, and microvesicles in yellow. In event 1, nucleocapsids are attached perpendicularly to a large, intact, globular intranuclear vesicle. The black boxes show different nucleocapsid bundles. In event 2, numerous nucleocapsids are attached, causing large vesicles to become elongated and spherical, and thereby creating a gap (indicated by the arrow) at one end. In event 3, nucleocapsids bind to concave (3a) and convex (3b) surfaces of arch-shaped membranes, with some microvesicles located nearby. In event 4, several bundles of nucleocapsids are enveloped into one ODV but they are not yet oriented parallel to each other. In event 5, the membrane of an ODV containing various nucleocapsids bundles invaginates to separate the bundles into new ODVs. The scale bars are 200 nm in events 1–4 and 100 nm in event 5. Cells were harvested at 36 h post-infection (p.i.) in events 1–3A and 4, and at 48 h p.i. in events 3B and 5. (B) Frequencies of ODVs at various events at the specified times. The blue, red, and green columns indicate ODVs in cells at 36, 48 and 72 h p.i. respectively.

throughout the RZ of the infected cells harvested at 36 h p.i., 48 h p.i. and 72 h p.i. Based on our observations, the ODV envelopment process can be classified into five events as follows:

(1) In event 1, nucleocapsids are attached perpendicularly to a large intact globular intranuclear vesicle (Fig. 4A, event 1). The diameter of this intact large vesicle is approximately 5-fold larger than the mean diameter of microvesicles. The area inside the large vesicle is more transparent than that of the surrounding area or inside ruptured microvesicles, indicating the environment inside is different from the outside and the vesicle is intact. Notably, the nucleocapsids on a given vesicle are not uniformly distributed and some are aggregated in bundles (Fig 4A, event 1). In each bundle, the nucleocapsids are oriented parallel to each other.

(2) In event 2, numerous nucleocapsids are attached to deformed and elongated spherical vesicles (Fig. 4A, event 2). Another important characteristic of this event is that the large vesicles rupture and gaps are observed in their membranes. The transparency inside these vesicles is similar to that of the surrounding area, revealing that the vesicles are ruptured. A primeval formed gap in the membrane of a microvesicle can be seen in tomography slices (Fig. 4A, event 2 arrow).

(3) In event 3, nucleocapsids binding to arch-shaped membranes are located at concave or convex surfaces (Fig. 4A, events 3a and 3b). The arch-shaped membranes are not large enough to entirely envelop all the attached nucleocapsids. However, microvesicles accumulate near or touching the membrane of enveloping ODVs (Fig. 3B), suggesting that microvesicles can replenish the arch-shaped membranes.

(4) Event 4 is a special stage of ODVs (Fig. 4A, event 4). Unlike the mature polyhedral ODVs, in which nucleocapsids in each ODV envelope are oriented parallel to each other, the arrangement of nucleocapsids at this stage is disorganized when observed by 2D conventional microscopy. From 3D analysis, we discover that the nucleocapsids are located in distinct bundles with different orientations, as mentioned in event 1. Nucleocapsids in each bundle are oriented parallel to each other.

(5) In event 5 (Fig. 4A, event 5), the envelopes of ODVs invaginate and nucleocapsids are separated into different ODVs such that all nucleocapsids in a given ODV are oriented parallel to each other.

Regarding the relationship between microvesicles and ODV membranes, although previous electron microscopy studies observed nucleocapsids attached to vesicle-like structures (Braunagel et al., 1996; Fraser, 1986), there is no convincing evidence that microvesicles are direct precursors of the ODV envelope. Here, we utilized ET to visualize capsids bundles attached to intact large microvesicles (Fig. 4A, event 1) and small microvesicles touching the arch-shaped membranes (Fig. 3B). This procedure reveals that microvesicles are the direct source of the ODV envelope. Moreover, there are two kinds of microvesicles: large (Fig. 4A, event 1) and small (Fig. 3B). These are derived from the same origin but play different roles in ODV envelopment. Large microvesicles are important for initiation of ODV envelopment, whereas small microvesicles are important for membrane enlargement in the enveloping ODV.

To determine the sequential steps involved in ODV envelopment, we quantified the proportion of ODVs at each event in each sample, which reflected the frequency of certain event in each sample. For this, we combined events 4 and 5 because it is difficult to distinguish between enveloping ODVs at event 4 and those at event 5 in 2D, and ET is not appropriate for the acquisition of large quantities of data.

In this analysis, enveloping ODVs at event 1 or 2 are rare, and we found 19 cases of event 1 and 21 cases of event 2 out of total 809 cases. Although we have to exclude the events 1 and 2 from these data analyses for their low frequency, we still have some evidences to infer these two steps as the begin steps in the model. Firstly, at the early infection (less than 24 h post-infection), we did not find the open membrane sheet without nucleocapsids binding that is similar with the membrane in events 3A and 3B. Secondly, it is easier to find the vesicles in various sizes without nucleocapsids attaching at 24 h.p.i and even several hours before 24 h.p.i. Thirdly, our statistics show that event 3A is more frequent in 36 h and event 3B is more frequent in 48 h. The curvature change of membrane hints that the capsids binding membranes undergo a flipping process, and it is reasonable for the vesicles from event 2 to event 3A. As the reasons above, the nucleocapsids should bind on the vesicles first.

The statistical analyses demonstrate that frequencies of event 3A at 36 h p.i. are highest, the frequencies have significant difference ($P=0.0018$) between 36 h and 72 h p.i.. Similar results show that frequencies of event 3B at 48 h and event 4+5 at 72 h are highest (Fig. 4B). (The P values of event 3B between 48 and 72 h p.i., and event 4+5 between 36 and 72 h p.i. are 0.0151 and 0.0043, respectively.) Thus enveloping ODVs at event 3A appear earlier than those at event 3B, whereas ODVs at event 4+5 appear much later. Therefore, we infer that ODV envelopment involves a series of sequential steps, namely, event 3A followed by event 3B followed by events 4 and 5. Enveloping ODVs at event 5 are attempting to form mature ODVs, meaning event 4 precedes event 5.

In summary, we deduced a model of ODV envelopment involving sequential steps (Fig. 1). First, several nucleocapsids bundles adhere to the large microvesicles (Fig. 1D). As more nucleocapsids bundles attach, the microvesicles are deformed and cleaved (Fig. 1E). Thereafter, expanding gaps cause the membranes of microvesicles to become arch-shaped (Fig. 1F, and G), and they gradually become inverted and envelop the attached nucleocapsids (Fig. 1H). During envelopment, the arch-shaped membranes continuously fuse with nearby microvesicles, meaning that the membranes expand and are eventually large enough to envelop all the nucleocapsids. Immature ODVs contain many nucleocapsids bundles that are not oriented parallel to each other. Thereafter, the membranes of immature ODVs invaginate (Fig. 1I), separating the bundles into mature ODVs (Fig. 1J). Subsequently, the nucleocapsids in each ODV are oriented parallel to each other, which is consistent with the observation that almost all polyhedral ODVs have nucleocapsids oriented parallel to each other (Kawamoto and Asayama, 1975). Electron tomography combined with sectioning of plastic-embedded samples reveals much more evidences in microvesicle formation and ODV envelopment. And using the snapshots in viral infection to give evidences of infection model is still widely accepted, for example, the Gamma-herpes virus life cycle model (Peng et al., 2010), the HIV entry model (Sougrat et al., 2007), and the Filovirus budding model (Welsch et al., 2010), yet the snapshots sometimes may unavoidably include some rare abortive intermediates. Therefore further validation of the mutants or inhibitors will be conducted in the future.

Comparing our results with previous studies of SNPVs (Stoltz et al., 1973), we find several distinct features of SNPV envelopment: 1) most intranuclear membranes are open membrane sheets, not vesicles; 2) the capsid binds open membrane sheets individually and capsids bundles are not observed in the nucleus; and 3) the membrane of the enveloping ODV seems large enough to cover the capsid. However, the mechanism underlying envelopment of single or multiple nucleocapsids requires further study.

Enveloped viruses mainly harvest their membranes in either of two ways. First, virions can bud through the plasma membrane and thereby be enveloped; this is true of the influenza virus (Nayak et al., 2009, 2004), various retroviruses (Morita and Sundquist, 2004), and alphaviruses (Martín et al., 2009; Martinez et al., 2014). Alternatively, virions can bud into the lumen of cellular cisterna and be released from the cell via exocytosis; this is true of the herpes simplex virus (Mettenleiter, 2002, 2004), flaviviruses (Martín et al., 2009), the hepatitis B virus (Ganem and Prince, 2004), and the hepatitis C virus (Mizuno et al., 1995). Compared with these viral envelopment strategies, the strategy adopted by ODV is rare, because its membranes are derived from intranuclear microvesicles, which are themselves from nuclear membranes (Beniya et al., 1998; Braunagel et al., 1996; Braunagel and Summers, 2007; Hong et al., 1994; Hu et al., 2010; Wei et al., 2014), and numerous nucleocapsids can be enveloped by one ODV. Elucidation of ODV morphogenesis can not only broaden our understanding of virology, but also provide structural information to study how nuclear membranes are seized by viruses and pathogens.

Materials and methods

Cells culture and viral infection

Sf9 insect cells, a *Spodoptera frugiperda* IPLB-Sf21-AE clonal isolate (Vaughn et al., 1977), were cultured at 27 °C in Grace's insect medium (Invitrogen Life Technologies) containing 10% fetal bovine serum, penicillin (100 units/ml), and streptomycin (100 μg/ml). When 80% confluent, cells were infected with AcMNPV at 27 °C with a multiplicity of infection of 36. The virus inoculum was incubated for 2 h at 27 °C and then replaced with fresh medium. Several plates of cells were treated at the same time in the same way. At the same time, control cells were treated with buffer instead of the virus inoculum. The infection start time was defined as when AcMNPV was mixed with the cells.

Sample preparation for electron microscopy

Infected cells at different time points p.i. as well as the corresponding control cells were washed with phosphate-buffered saline (PBS), detached and pelleted at 500*g* for 10 min at 4 °C. The cells were fixed in 3% glutaraldehyde and 2% paraformaldehyde prepared in 0.1 M PBS (pH 7.2) for 12 h at 4 °C, and then treated with 1% osmium tetroxide for 1.5 h at room temperature. Thereafter samples were gradient dehydrated and embedded in Spurr (Sigma-Aldrich Co., USA). Sections were cut and stained with aqueous uranyl acetate and lead citrate (Qinfen et al., 2004). For ET, 350–450 nm-thick sections were prepared and colloidal gold particles (15 nm in diameter) were applied to the both sides of the semi-thick slices as fiducial markers.

ET and image processing

ET data were collected using a JEM 2010 microscope operated at 200 kV as previously described (Huang et al., 2010). Eighty-two tilt series were collected with a 2K × 4K CCD camera (Gatan 832) and the tilt angle was manually operated from −60° to 60° with 2° interval. The final Å/pixel of the tomograms were among 0.944 nm, 0.755 nm, 0.629 nm, 0.503 nm and 0.378 nm. The *IMOD* package (Kremer et al., 1996) was used for reconstruction, segmentation, and rendering.

Statistical analysis of microvesicles

All microvesicle data were collected from the 3D tomograms. The diameters of microvesicles inside and outside of foci were statistically analyzed using the SAS program (version 8.1, 1999–2000, SAS Institute Inc., Cary, NC) (Zhu et al., 2014). Data were compared using

the Student *t*-test. *IMOD* tools were used to measure the diameter of vesicles inside and outside of the foci (Kremer et al., 1996).

Quantification of frequencies of ODVs at various events of the envelopment process

Cells harvested at 36 h, 48 h, and 72 h p.i. (50 cells per time point) were observed by conventional TEM and the number of ODVs at various events was counted. The proportions of ODVs at each event in each sample were calculated. Thereafter, the various frequencies were compared among the time posts. Events 4 and 5 were combined in this quantification.

The statistical analysis of the frequencies data was performed by one-way analysis of variance (ANOVA) followed by a Ducan's multiple range tests for multiple comparisons. Significant differences were considered at $P < 0.05$. All data analysis was performed using SAS program (version 8.1, 1999–2000, SAS Institute Inc, Cary, NC).

Acknowledgments

This research was supported by the National Natural Science Foundation of China (31070654), the Science Foundation of the State Key Laboratory of Biocontrol (SKLBC10B05). We thank a lot Dr. Meijing Yuan, Denghui Wei and Mr. Dong Chen for their great helps on the sample preparations and many suggestions on the experiments.

References

Beniya, H., Braunagel, S.C., Summers, M.D., 1998. *Autographa californica* nuclear polyhedrosis virus: subcellular localization and protein trafficking of BV/ODV-E26 to intranuclear membranes and viral envelopes. Virology 240, 64–75.

Braunagel, S., Elton, D., Ma, H., Summers, M., 1996. Identification and analysis of an *Autographa californica* nuclear polyhedrosis virus structural protein of the occlusion-derived virus envelope: *ODV-E56*. Virology 217, 97–110.

Braunagel, S.C., Summers, M.D., 1994. A*utographa californica* nuclear polyhedrosis virus, PDV, and ECV viral envelopes and nucleocapsids: structural proteins, antigens, lipid and fatty acid profiles. Virology 202, 315–328.

Braunagel, S.C., Summers, M.D., 2007. Molecular biology of the baculovirus occlusion-derived virus envelope. Curr. Drug Targets 8, 1084–1095.

Engelhard, E., Kam-Morgan, L., Washburn, J., Volkman, L., 1994. The insect tracheal system: a conduit for the systemic spread of *Autographa californica* M nuclear polyhedrosis virus. Proc. Natl. Acad. Sci. USA 91, 3224–3227.

Fraser, M., 1986. Ultrastructural observations of virion maturation in *Autographa californica* nuclear polyhedrosis virus infected *Spodoptera frugiperda* cell cultures. J. Ultrastruct. Mol. Struct. Res. 95, 189–195.

Ganem, D., Prince, A.M., 2004. Hepatitis B virus infection—natural history and clinical consequences. N. Engl. J. Med. 350, 1118–1129.

Hong, T., Braunagel, S.C., Summers, M.D., 1994. Transcription, translation, and cellular localization of PDV-E66: a structural protein of the PDV envelope of *Autographa californica* nuclear polyhedrosis virus. Virology 204, 210–222.

Hong, T., Summers, M.D., Braunagel, S.C., 1997. N-terminal sequences from *Autographa californica* nuclear polyhedrosis virus envelope proteins ODV-E66 and ODV-E25 are sufficient to direct reporter proteins to the nuclear envelope, intranuclear microvesicles and the envelope of occlusion derived virus. Proc. Natl. Acad. Sci. USA 94, 4050–4055.

Hou, D., Zhang, L., Deng, F., Fang, W., Wang, R., Liu, X., Guo, L., Rayner, S., Chen, X., Wang, H., 2013. Comparative proteomics reveal fundamental structural and functional differences between the two progeny phenotypes of a baculovirus. J. Virol. 87, 829–839.

Hu, Z., Yuan, M., Wu, W., Liu, C., Yang, K., Pang, Y., 2010. Autographa californica multiple nucleopolyhedrovirus ac76 is involved in intranuclear microvesicle formation. J. Virol. 84, 7437–7447.

Huang, Z., Chen, M., Li, K., Dong, X., Han, J., Zhang, Q., 2010. Cryo-electron tomography of *Chlamydia trachomatis* gives a clue to the mechanism of outer membrane changes. J. Electron Microsc. 59, 237–241.

Jehle, J.A., Blissard, G., Bonning, B., Cory, J., Herniou, E., Rohrmann, G., Theilmann, D., Thiem, S., Vlak, J., 2006. On the classification and nomenclature of baculoviruses: a proposal for revision. Arch. Virol. 151, 1257–1266.

Kawamoto, F., Asayama, T., 1975. Studies on the arrangement patterns of nucleocapsids within the envelopes of nuclear-polyhedrosis virus in the fat-body cells of the brown tail moth, *Euproctis similis*. J. Invertebr. Pathol. 26, 47–55.

Kawamoto, F., Kumada, N., Kobayashi, M., 1977. Envelopment of the nuclear polyhedrosis virus of the oriental tussock moth, *Euproctis subflava*. Virology 77, 867–871.

Knudson, D., Harrap, K., 1976. Replication of a nuclear polyhedrosis virus in a continuous cell culture of *Spodoptera frugiperda*: microscopy study of the sequence of events of the virus infection. J. Virol. 17, 254–268.

Kremer, J.R., Mastronarde, D.N., McIntosh, J.R., 1996. Computer visualization of three-dimensional image data using IMOD. J. Struct. Biol. 116, 71–76.

MacKinnon, E., Henderson, J., Stoltz, D., Faulkner, P., 1974. Morphogenesis of nuclear polyhedrosis virus under conditions of prolonged passage in vitro. J. Ultrastruct. Res. 49, 419–435.

Martín, C.S.-S., Liu, C.Y., Kielian, M., 2009. Dealing with low pH: entry and exit of alphaviruses and flaviviruses. Trends Microbiol. 17, 514–521.

Martinez, M.G., Snapp, E.-L., Perumal, G.S., Macaluso, F.P., Kielian, M., 2014. Imaging the alphavirus exit pathway. J. Virol. 88, 6922–6933.

McCarthy, C.B., Dai, X., Donly, C., Theilmann, D.A., 2008. *Autographa californica* multiple nucleopolyhedrovirus *ac142*, a core gene that is essential for BV production and ODV envelopment. Virology 372, 325–339.

Mettenleiter, T.C., 2002. Herpesvirus assembly and egress. J. Virol. 76, 1537–1547.

Mettenleiter, T.C., 2004. Budding events in herpesvirus morphogenesis. Virus Res. 106, 167–180.

Mizuno, M., Yamada, G., Tanaka, T., Shimotohno, K., Takatani, M., Tsuji, T., 1995. Virion-like structures in HeLa G cells transfected with the full-length sequence of the hepatitis C virus genome. Gastroenterology 109, 1933–1940.

Morita, E., Sundquist, W.I., 2004. Retrovirus budding. Annu. Rev. Cell Dev. Biol. 20, 395–425.

Nayak, D.P., Balogun, R.A., Yamada, H., Zhou, Z.H., Barman, S., 2009. Influenza virus morphogenesis and budding. Virus Res. 143, 147–161.

Nayak, D.P., Hui, E.K.-W., Barman, S., 2004. Assembly and budding of influenza virus. Virus Res. 106, 147–165.

Peng, L., Ryazantsev, S., Sun, R., Zhou, Z.H., 2010. Three-dimensional visualization of gammaherpesvirus life cycle in host cells by electron tomography. Structure 18, 47–58.

Qinfen, Z., Jinming, C., Xiaojun, H., Huanying, Z., Jicheng, H., Ling, F., Kunpeng, L., Jingqiang, Z., 2004. The life cycle of SARS coronavirus in Vero E6 cells. J. Med. Virol. 73, 332–337.

Slack, J., Arif, B.M., 2007. The baculoviruses occlusion-derived virus: virion structure and function. Adv. Virus Res. 69, 100.

Sougrat, R., Bartesaghi, A., Lifson, J.D., Bennett, A.E., Bess, J.W., Zabransky, D.J., Subramaniam, S., 2007. Electron tomography of the contact between T cells and SIV/HIV-1: implications for viral entry. PLoS Pathog. 3, e63.

Stoltz, D., Pavan, C., Da Cunha, A., 1973. Nuclear polyhedrosis virus: a possible example of de novo intranuclear membrane morphogenesis. J. Gen. Virol. 19, 145–150.

Summers, M.D., Volkman, L.E., 1976. Comparison of biophysical and morphological properties of occluded and extracellular nonoccluded baculovirus from in vivo and in vitro host systems. J. Virol. 17, 962–972.

Tanada, Y., Hess, R.T., 1976. Development of a nuclear polyhedrosis virus in midgut cells and penetration of the virus into the hemocoel of the armyworm, *Pseudaletia unipuncta*. J. Invertebr. Pathol. 28, 67–76.

Vaughn, J., Goodwin, R., Tompkins, G., McCawley, P., 1977. The establishment of two cell lines from the insect *Spodoptera frugiperda* (Lepidoptera; Noctuidae). In Vitro 13, 213–217.

Wei, D., Wang, Y., Zhang, X., Hu, Z., Yuan, M., Yang, K., 2014. *Autographa californica* nucleopolyhedrovirus Ac76: a dimeric type II integral membrane protein that contains an inner nuclear membrane-sorting motif. J. Virol. 88, 1090–1103.

Welsch, S., Kolesnikova, L., Krahling, V., Riches, J.D., Becker, S., Briggs, J.A., 2010. Electron tomography reveals the steps in filovirus budding. PLoS Pathog. 6, e1000875.

Welsch, S., Müller, B., Kräusslich, H.-G., 2007. More than one door–budding of enveloped viruses through cellular membranes. FEBS Lett. 581, 2089–2097.

Williams, G.V., Faulkner, P., 1997. Cytological changes and viral morphogenesis during baculovirus infection. In: Lois, K. Miller (Ed.), The Baculoviruses. Plenum Press, New York, NY, pp. 61–107.

Young, J., MacKinnon, E., Faulkner, P., 1993. The architecture of the virogenic stroma in isolated nuclei of *Spodoptera frugiperda* cells in vitro infected by *Autographa californica* nuclear polyhedrosis virus. J. Struct. Biol. 110, 141–153.

Yuan, M., Huang, Z., Wei, D., Hu, Z., Yang, K., Pang, Y., 2011. Identification of Autographa californica nucleopolyhedrovirus ac93 as a core gene and its requirement for intranuclear microvesicle formation and nuclear egress of nucleocapsids. J. Virol. 85, 11664–11674.

Yuan, M., Wu, W., Liu, C., Wang, Y., Hu, Z., Yang, K., Pang, Y., 2008. A highly conserved baculovirus gene p48 (ac103) is essential for BV production and ODV envelopment. Virology 379, 87–96.

Zhu, H., Li, H., Wang, P.u., Chen, M., Huang, Z., Li, K., Li, Y., He, J., Han, J., Zhang, Q., 2014. Persistent and acute chlamydial infections induce different structural changes in the Golgi apparatus. Int. J. Med. Microbiol. 304, 577–585.